Clays and Clay Minerals, Vol. 65, No. 6, 378–386, 2017.

MOLECULAR DYNAMICS SIMULATION OF ALKYLAMMONIUM-INTERCALATED VERMICULITES

CHENG CHEN, XIANDONG LIU*, YINGCHUN ZHANG, CHI ZHANG, AND XIANCAI LU

State Key Lab for Mineral Deposits Research, School of Earth Sciences and Engineering, Nanjing University, Nanjing, 210046, P. R. China

Abstract—In order to understand the microscopic properties of alkylammonium-intercalated vermiculites, molecular dynamics simulations employing the clayff-CVFF force field were performed to obtain the interlayer structures and dynamics. The layering behavior of alkyl chains was uncovered. With the model used in the present study (1.2 *e* per unit cell), the alkyl chains formed monolayers with carbon-chain lengths of C_6, bilayers from C_7 to C_{10}, and pseudo-trimolecular layers from C_{15} to C_{18}. Intermediate states also existed between bilayer and pseudo-trimolecular layer states from C_{11} to C_{14}. The ammonium groups had two locations: most ammonium groups were located over the six-member rings (~90%), and the rest above the substitution sites (~10%). The ammonium groups interacted with the vermiculite surface through H bonds between ammonium H atoms and surface O atoms. The ammonium groups were fixed firmly on surfaces and, therefore, had very low mobility. The alkyl chains were slightly more mobile. The similarities and differences between alkylammonium-intercalated vermiculites and smectites were revealed. The layering behaviors of alkyl chains were similar in alkylammonium-intercalated vermiculites and smectites: the alkyl chain behavior was controlled by both the amount of layer charge and the carbon chain length. The distributions of ammonium groups, however, were different, caused by the layer-charge distribution in vermiculites being different from that in smectites. The atomic-level results derived in the present study will be useful for future research into and the applications of organo-vermiculites.

Key Words—Alkylammonium, Intercalation, Interlayer Structures, Mobility, Molecular Dynamics, Vermiculites.

INTRODUCTION

Vermiculite is a 2:1 type clay mineral with negative layer charge, which is caused by the isomorphic substitution of Al for Si in the tetrahedral sheet (Brigatti *et al*., 2013). Vermiculite is used widely in many industrial processes because of its remarkable physical and chemical properties: low thermal conductivity and density, refractory behavior, and large cation exchange capacity (Harvey and Lagaly, 2013). Vermiculite is quite different from smectite. Smectite is generally a dioctahedral clay mineral while vermiculite belongs to the trioctahedral type; the layer charge of vermiculite (~1.2−1.8 *e* per unit cell) is greater than that of smectite (~0.6−1.2 *e* per unit cell); isomorphic substitutions occur mostly in the tetrahedral sheets for vermiculite but in the octahedral sheets for smectite.

In nature, the negative layer charge of clay minerals is usually balanced by inorganic cations such as Na^+ and Ca^{2+}. They can be replaced by organic cations through ion exchange, forming organic-clay complexes, known as organoclays (Lagaly *et al*., 2013). Organoclays have many applications in industry due to the excellent material properties compared with natural clays, *e.g.* organophilicity, increased strength and heat resistance, and decreased gas permeability and flammability (Lagaly *et al*., 2013). Among various organoclays, the alkylammonium-intercalated clays draw significant attention because they can be prepared easily and the molecular structures of alkylammonium species are relatively simple. The intercalation of alkylammonium ions changes clays from organophobic to organophilic and expands the interlayer space; this means that the uptake capacity for organic matter is improved. For this reason, alkylammonium-intercalated clays have been employed to remove organic contaminants from water (Lee *et al*., 1989; Carrizosa *et al*., 2004; Nguemtchouin *et al*., 2015). The alkylammonium species are also important in the preparation of clay-polymer nanocomposites (CPNs) (Lagaly *et al*., 2013; Mykola *et al*., 2016; Al-Samhan *et al*., 2017).

Extensive experiments have been carried out to study the interlayer structures of alkylammonium-intercalated clays. X-ray diffraction (XRD) measurements show that the basal spacings of alkylammonium-intercalated smectites increase in steps, and the arrangement of the intercalated alkylammonium ions depends on the layer charge and the alkyl-chain length (Weiss, 1963; Lagaly, 1981; Laird *et al*., 1989; Janek and Smrcok, 1999). Fourier-transform infrared spectroscopy (Vaia *et al*., 1994; Osman *et al*., 2000, 2002, 2004; Zhu *et al*., 2005;

* E-mail address of corresponding author:
xiandongliu@nju.edu.cn
DOI: 10.1346/CCMN.2017.064070

This paper was originally presented during the 3rd Asian Clay Conference, November 2016, in Guangzhou, China.

https://doi.org/10.1346/CCMN.2017.064070 Published online by Cambridge University Press

Li *et al*., 2008; Sarkar *et al*., 2011; Pazos *et al*., 2015), nuclear magnetic resonance spectroscopy (Wang *et al*., 2000; Osman *et al*., 2002, 2004; Zhu *et al*., 2005; Wen *et al*., 2006; Pazos *et al*., 2015), and near-infrared spectroscopy (Jankovič *et al*., 2015; Madejová *et al*., 2016) techniques have also been used to investigate the conformations of alkylammonium species.

In recent decades, molecular simulation has been applied to investigate clay minerals, and this technique has proven to be powerful because it can complement experimental results (Escamilla-Roa *et al*., 2016; Ferrage, 2016; Kalinichev *et al*., 2016; Szczerba *et al*., 2016). Many simulation studies have been conducted to investigate the interlayer structures and dynamics of alkylammonium-intercalated clays (Zeng *et al*., 2003, 2004; He *et al*., 2005; Tambach *et al*., 2006; Liu *et al*., 2007, 2009; Zhao and Burns, 2012; Bardziński, 2014; Scholtzová *et al*., 2016).

Most of the research, however, has focused on alkylammonium-intercalated smectites while less attention has been paid to vermiculite. For instance, the evolution of basal spacings of alkylammonium-intercalated vermiculite as a function of carbon-chain length and the layering behavior of alkylammonium were investigated by Lagaly (1982) using XRD measurements. The swelling and conformations of alkylammonium intercalated in vermiculite were investigated by Tambach *et al*. (2006) but the carbon-chain lengths of alkylammonium only ranged from 5 to 13 and the very long chains were not involved. In both studies, the authors were less concerned with the interactions of alkylammonium ions with clay mineral surfaces and more about the layering behavior of alkylammonium; dynamic information was not considered.

The different structures and layer charges between vermiculites and smectites may lead to different properties in the corresponding organoclays. How do the alkylammonium species behave in the interlayer space of vermiculite? Are they different? These questions have yet to be answered. The purpose of the present study was to help answer those questions about the interlayer structures and dynamics of alkylammonium-intercalated vermiculite using molecular dynamics (MD) simulations with the clayff-CVFF force field (Cygan *et al*., 2004; Dauber-Osguthorpe *et al*., 1988). Of particular interest were the evolution of basal spacings as a function of carbon-chain lengths ranging from C_6 to C_{18} and the validation of the reliability of the clayff-CVFF force field method.

METHODS

To accomplish the objective of this study, four representative systems, C_6, C_{10}, C_{13}, and C_{18} ammonium-intercalated vermiculites, were chosen to investigate the layering behavior of alkyl chains, the mobility of interlayer species, and the interaction between alkylammonium ions and clay surfaces.

The organoclay model

The clay model was modified from the prototype introduced by Gruner (1934), with a chemical formula of $X_{1.2}(Si_{6.8}Al_{1.2})Mg_6O_{20}(OH)_4$, where X stands for the interlayer compensation cation. The clay's framework had a negative layer charge of 1.2 e per unit cell. The isomorphic substitutions were constrained to obey Loewenstein's (1954) rule, *i.e.* two substitution sites cannot be adjacent. The supercell used for simulation consisted of two clay platelets, and each of them contained 40 unit cells: ten in the x dimension and four in the y dimension. The model included two interlayer spaces, and 48 alkylammonium ions were placed randomly in each of them to neutralize the negative charges of the clay framework (Figure 1). The basal surface area was 53.10 Å × 36.80 Å and the thickness of the clay platelet was ~6.50 Å. To accommodate the alkylammonium ions with long chains, the initial basal spacing was set at 39 Å.

Simulation details

All MD simulations were carried out using the DL_POLY_2.20 package (Smith and Forester, 1996). In the present study, the clayff-CVFF force field (Cygan *et al*., 2004; Dauber-Osguthorpe *et al*., 1988) was employed to describe the interatomic interactions, *i.e.* clayff for vermiculite and CVFF for the intercalated organic ions. In clayff-CVFF, the total energy can be expressed as (Cygan, 2001; Perry *et al*., 2006):

$$E_{\text{total}} = E_{\text{Coul}} + E_{\text{VDW}} + E_{\text{bond stretch}} + E_{\text{bond bend}} + E_{\text{torsion}} \quad (1)$$

Here E_{coul}, E_{VDW}, $E_{\text{bond stretch}}$, $E_{\text{bond bend}}$, and E_{torsion} are the energy contribution of coulombic interaction, the Van der Waals interaction, the bond stretching, the bond bending, and the dihedral torsion, respectively. For vermiculite, only the first three terms were taken into account according to clayff, and all five terms were applied to the intercalated alkylammonium ions according to CVFF. A cutoff of 12.0 Å was used for the short-range Van der Waals interaction in the simulation, and the coulombic interaction was evaluated by the Ewald summation with a precision of 1.0×10^{-6}.

The isothermal-isobaric (NPT) (constant particle numbers, pressure, and temperature) simulations for the systems intercalated by alkylammonium ions with different alkyl chain lengths (ranging from 6 to 18) were performed at 298K and 1 atm to obtain the swelling curve. All NPT simulations were carried out first with an equilibration stage of 1 ns, followed by a 1 ns production stage to record the results. To study the microscopic structures and mobility of interlayer species, other 2 ns simulations were performed in the canonical ensembles (NVT) (constant particle numbers, volume, and temperature) at 298K for the representative C_6, C_{10}, C_{13}, and C_{18} systems following the previous NPT simulations. In all simulations, the time step was set at 1.0 fs and an

https://doi.org/10.1346/CCMN.2017.064070 Published online by Cambridge University Press

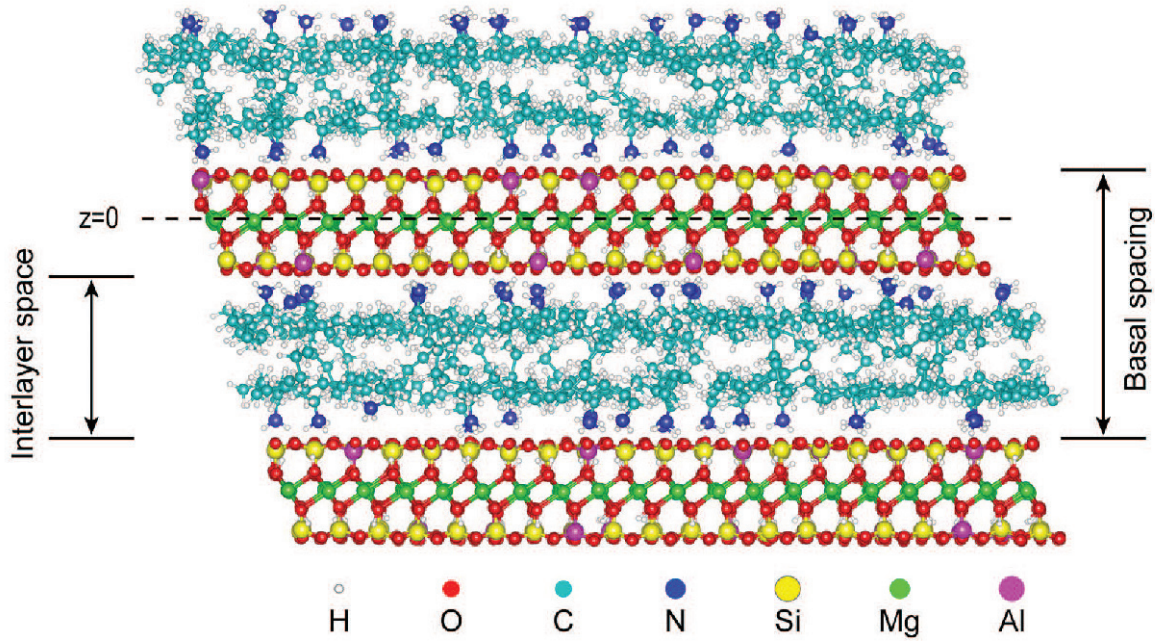


Figure 1. Snapshot of vermiculite intercalated by C_{10}-alkylammoniums.

interval of 100 fs was used for recording trajectories. All atoms were allowed to move.

RESULTS

Basal spacings

The swelling curves of simulated and experimental results were plotted together for comparison (Figure 2). The experimental data were from XRD analysis of alkylammonium-intercalated vermiculite (Lagaly, 1982) with a layer charge (1.22 *e* per unit cell) similar to the present model (1.2 *e* per unit cell). The differences between simulated and experimental basal spacings were <1.0 Å, except for C_{16} (1.1 Å) and C_{17} (2.2 Å). The simulated results agreed in essence with experimental data, indicating that the combined clayff-CVFF force field was applicable for this system.

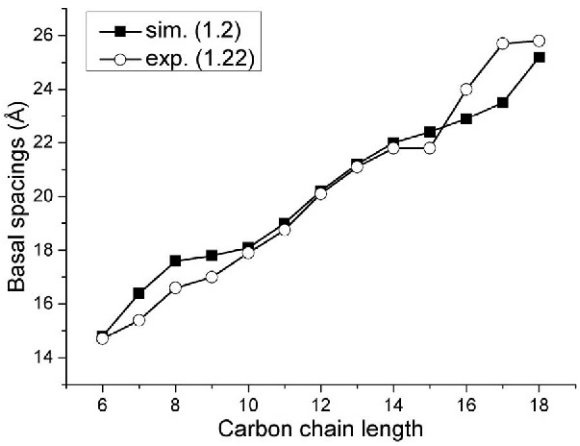


Figure 2. Swelling curves of alkylammonium-vermiculite. Experimental data are from Lagaly (1982). The numbers in the parentheses are the layer charge per unit cell. The error bars are smaller than the symbol size. The lines between the data are used to guide the eye.

The swelling curves showed that the basal spacings increased in step with the carbon-chain length. This was also found by Lagaly *et al.* (2013) for low-charge vermiculites (layer charge $\leqslant$1.2 *e* per unit cell). The first plateau occurred from C_7 to C_{10}, and the other from C_{15} to C_{17}. The two plateaus represented monolayer and bilayer configurations of the alkyl chains, respectively, described in detail below.

Density distributions in the z direction

All interlayer species presented clear peaks in the density distribution profiles of the four representative systems (Figure 3). The ammonium nitrogen atoms all showed two peaks in each interlayer space of the four systems, and they were close to the clay surfaces. The different peaks of carbon chains in the C_6, C_{10}, C_{13}, and C_{18} systems revealed the layering behavior. In the C_6 system, the two single peaks stood for the monolayer configurations of the alkyl chains (see Figures 3a, 4a). In the C_{10} system, the appearance of double peaks in each interlayer space denoted the bilayer configurations (Figures 3b, 4b). As for the C_{18} system, the three peaks in each interlayer space indicated the formation of pseudo-trimolecular layers (Figures 3d, 4d). The peaks of carbon atoms in the C_{13} system indicated the intermediate state between bilayer and pseudo-trimolecular layer configurations (Figures 3c, 4c).

https://doi.org/10.1346/CCMN.2017.064070 Published online by Cambridge University Press

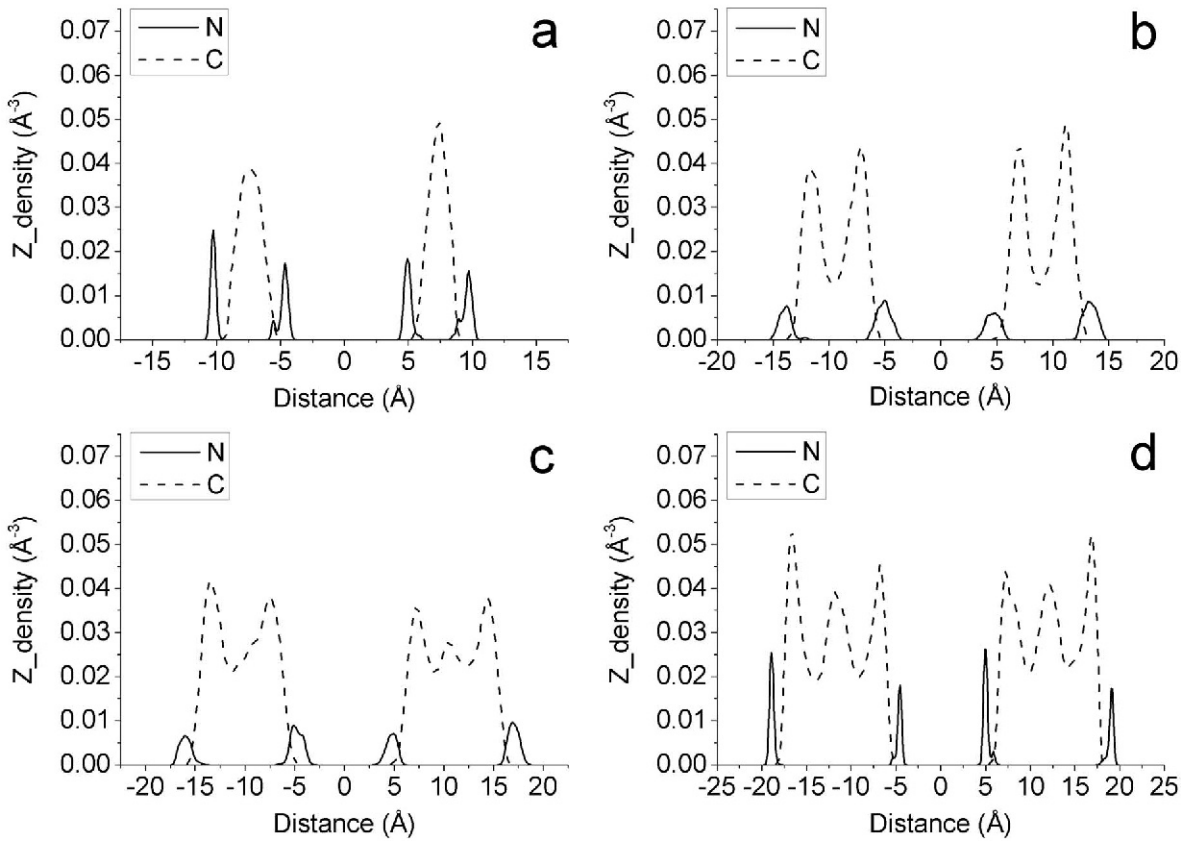


Figure 3. Density distribution profiles of interlayer atomic species in the organoclays of the four selected carbon chain lengths: (a) C_6; (b) C_{10}; (c) C_{13}; and (d) C_{18}.

For monolayer and bilayer configurations, the alkyl-chain axes were parallel to the basal plane. For pseudo-trimolecular layer configurations, the part close to the head group was parallel to the basal plane while the other part of the alkyl chain was not because of the formation of kinks (Lagaly *et al*., 2013). For the intermediate state, some alkylammonium ions were arranged in bilayer configurations while the others were in pseudo-trimolecular layer configurations.

The location of ammonium groups

Two locations of ammonium groups (Figure 5) were identified from the detailed analyses of trajectories. A minority of ammonium groups (~10%) were located above the Al substitution sites. Most ammonium groups (~90%), however, were located above the six-member rings. The ammonium groups interacted with the vermiculite surface through H bonds between ammonium H atoms and surface O atoms. The ammonium groups over the substitution sites formed H bonds through ammonium H atoms and the three O atoms attached to the same Al atom (Figure 6a), while the others formed H bonds through ammonium H atoms and the three O atoms of a six-member ring (Figure 6b). A ratio of 1:9 for the two locations of ammonium groups indicated that the latter structure was more stable.

Mean square displacements (MSDs)

The mean square displacements (MSDs) of the ammonium and alkyl groups of the four systems are shown in Figure 7. The MSD of the alkyl groups in the C_6 system (~0.7 Å^2) is the smallest among the four systems. The MSDs of the alkyl groups are similar in the C_{10}, C_{18}, and C_{13} systems, 1.60 Å^2, 2.0 Å^2, and 3.0 Å^2, respectively. The MSDs of the ammonium groups were smaller than that of the alkyl groups, and they had almost the same value of 0.2 Å^2 in the four systems. The small MSDs of alkyl groups and ammonium groups indicated that their motions were very restricted, and hence the Einstein relation (Allen and Tildesley, 1987; Chang *et al*., 1997) was not applicable to calculate the diffusion coefficients.

DISCUSSION

Interlayer structure

The layering behavior of alkyl chains was deduced from the swelling curves and density distribution

https://doi.org/10.1346/CCMN.2017.064070 Published online by Cambridge University Press

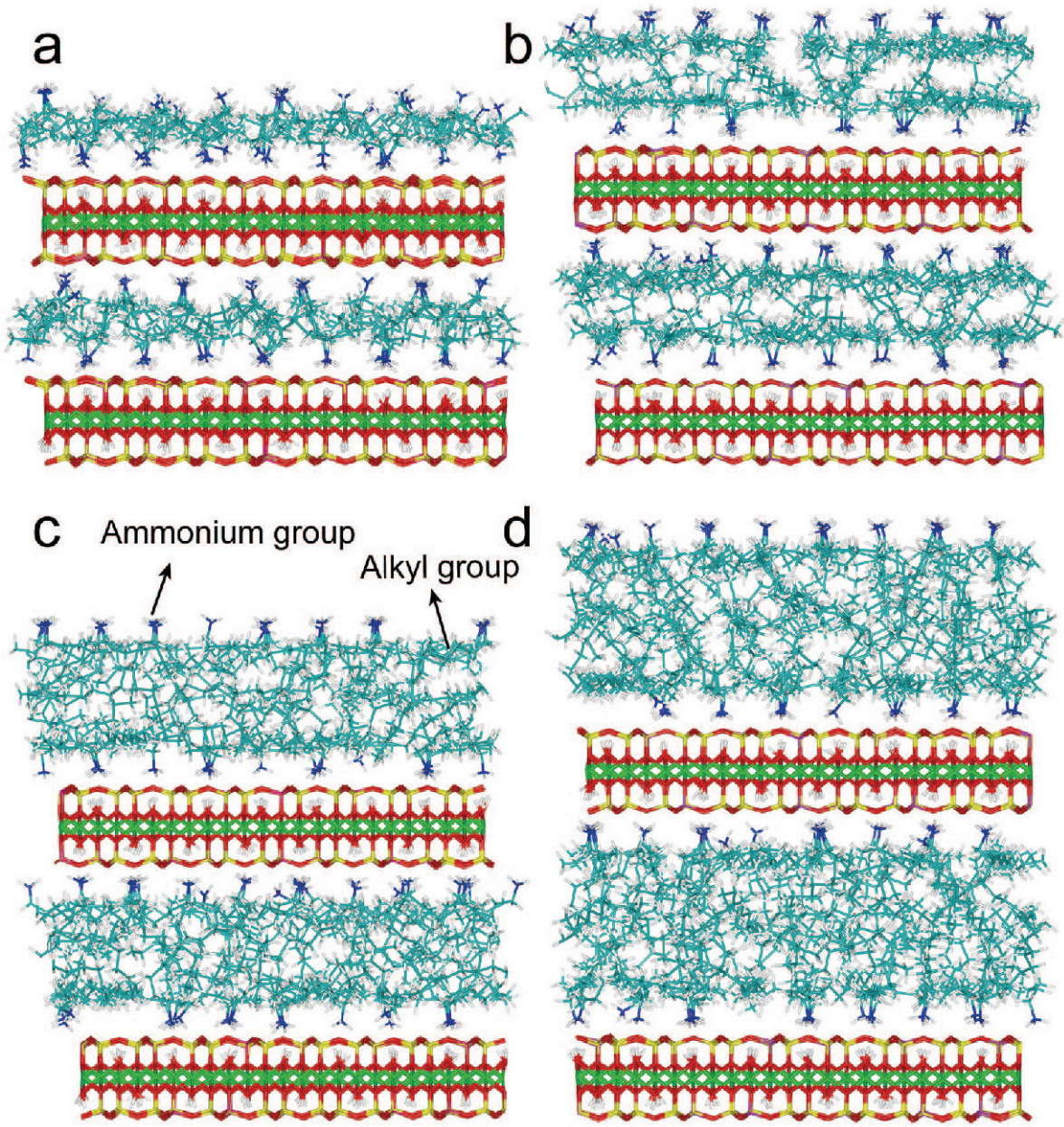


Figure 4. Snapshots of vermiculite intercalated by: (a) C_6; (b) C_{10}; (c) C_{13}; and (d) C_{18} ammoniums. Color scheme: Mg = green, Si = orange, Al = pink, O = red, H = white, C = brown, N = blue.

profiles. For C_6, the alkyl chains formed monolayers. The alkyl chains formed bilayers as the carbon chain lengths increased from C_7 to C_{10}, and pseudo-trimolecular layers when the carbon chain lengths ranged from C_{15} to C_{18}. The intermediate states between bilayer and pseudo-trimolecular layer existed from C_{11} to C_{14}.

The layering behavior of alkylammonium intercalated in vermiculites agreed well with those in smectites with the same amount of layer charge (Lagaly *et al*., 2013). The layer-charge distribution, therefore, has little influence on the layering behavior and the amount of layer charge is the key factor controlling the layering behavior of the intercalated alkylammonium ions. The layering behavior of alkylammonium intercalated in smectites as a function of layer charge and carbon-chain length is also applicable to other alkylammonium-intercalated clays.

The layering behavior of alkylammonium intercalated into smectites was different from the results for vermiculite according to the results of the studies by Liu *et al*. (2007) and Tambach *et al*. (2006). The alkylammonium ions formed monolayers up to a carbon-chain

https://doi.org/10.1346/CCMN.2017.064070 Published online by Cambridge University Press

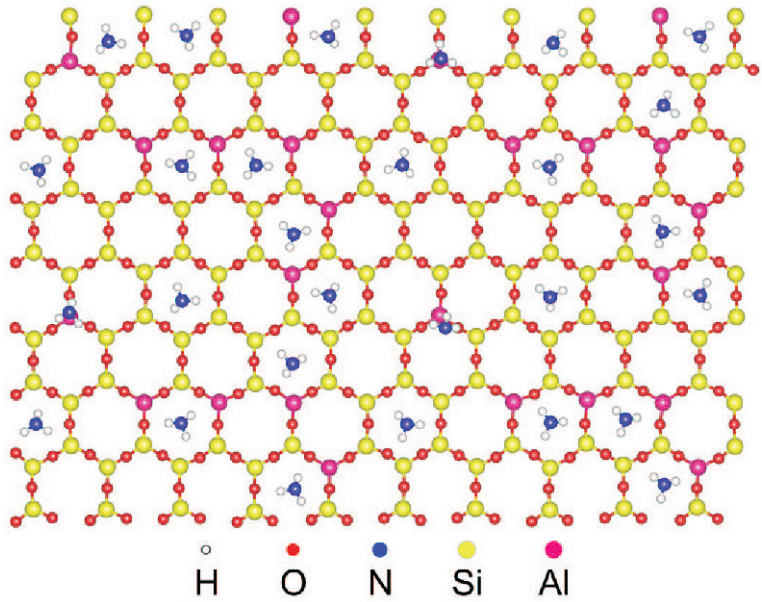


Figure 5. Snapshot of vermiculite intercalated by C_{10} ammonium, viewed from the direction perpendicular to the basal surface.

length of 12 and bilayers for the longer chains, but pseudo-trimolecular layers did not appear in the studies of those authors. The different amounts of layer charge between vermiculites (1.2 *e* per unit-cell) and smectites (0.625 *e* per unit-cell) are responsible for this difference.

As mentioned above, the ammonium groups had two locations: above the substitution sites and above the six-member rings. The ammonium groups in both locations interacted with the vermiculite surface through H bonds between ammonium H atoms and surface O atoms. The cases were different for alkylammonium and poly (propylene oxide)-ammonium intercalated in smectites (Heinz *et al*., 2005; Liu *et al*., 2007; Greenwell *et al*., 2005), where only the second situation was observed; all ammonium groups were located above the six-member rings. This was caused by the difference of substitution sites between vermiculites and smectites; the isomorphic substitutions of vermiculites mainly happen in the tetrahedral sheets, but in the octahedral sheets for smectites. The substitutions in the tetrahedral sheets make the charges of the three O atoms connected to the Al atom more negative and, thus, have greater attraction to the ammonium groups. This led some ammonium groups to locate above the substitution sites. In alkylammonium-intercalated vermiculite, however, the ammonium groups locating above the substitution sites constituted just 10% of the ammonium groups overall, so the six-member rings were still the most important locations for ammonium groups.

Mobility of interlayer species

The small MSDs of ammnonium and alkyl groups indicated that their motions were very restricted. As discussed above, the ammonium groups were fixed firmly over the two locations and, therefore, had very low mobility. The alkyl groups were slightly more mobile.

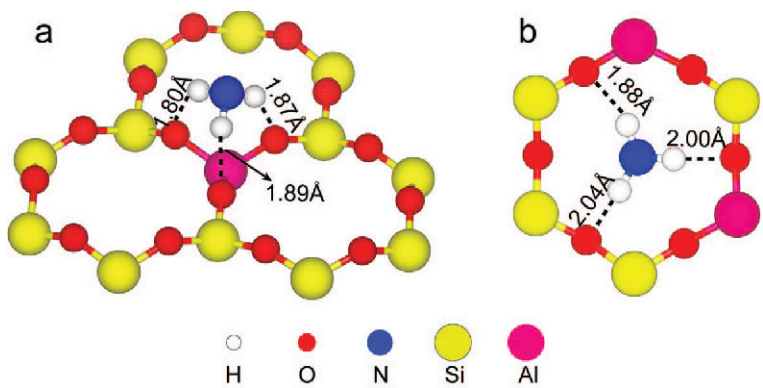


Figure 6. Two different locations of ammonium groups: (a) over the substitution site; (b) over the six-member ring.

https://doi.org/10.1346/CCMN.2017.064070 Published online by Cambridge University Press

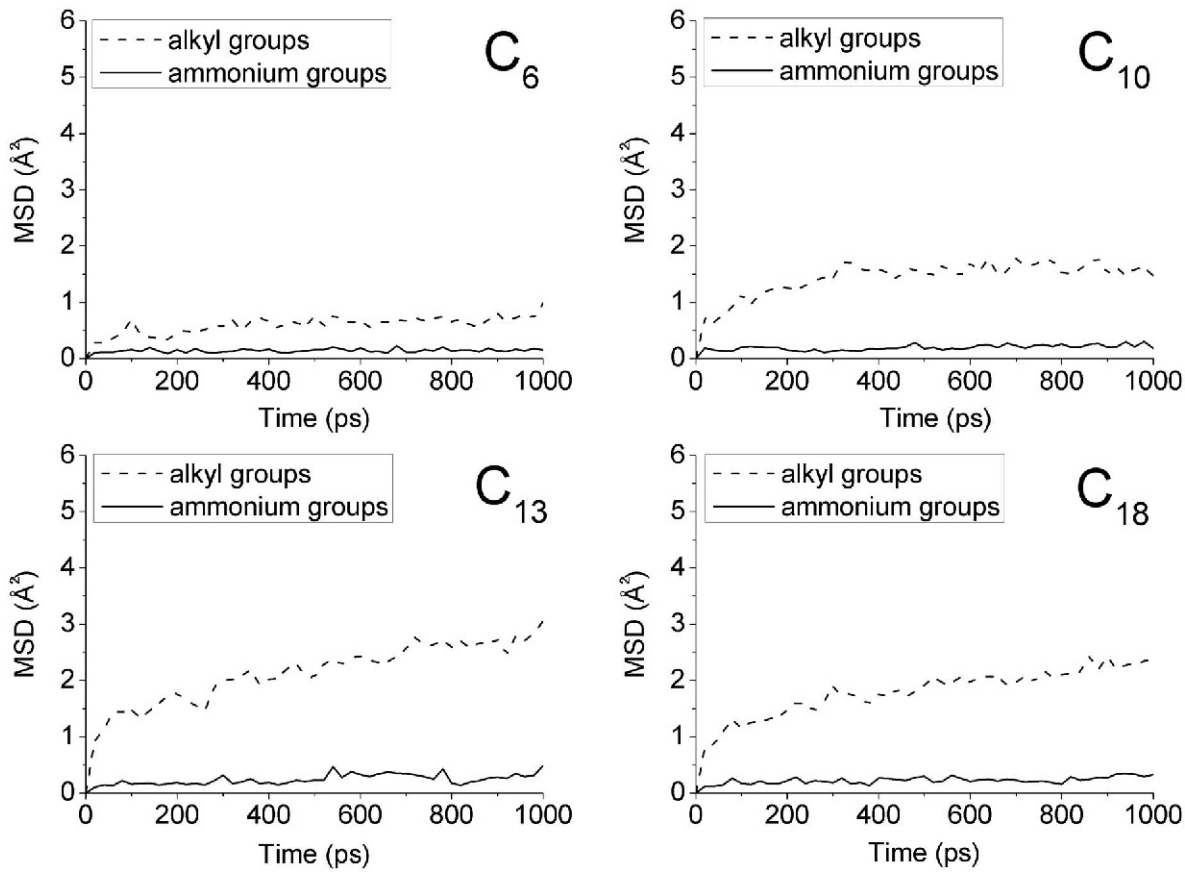


Figure 7. Mean square displacements of interlayer species in the organoclays of the four selected systems: C_6, C_{10}, C_{13}, and C_{18}.

This was very similar to the results of alkylammonium intercalated into smectites (Liu *et al*., 2007), but the MSDs of the alkyl groups in alkylammonium-intercalated vermiculites in this research were smaller than those in alkylammonium-intercalated smectites in previous simulations by Liu *et al* (2007). For example, the MSDs of the alkyl groups in the C_{18} systems were 2.0 Å^2 and 7.5 Å^2 in the present study and in the research of Liu *et al* (2007), respectively. The larger layer charge of vermiculites compared to smectites resulted in more alkylammonium ions in the interlayer space. This may cause the relatively low mobility of alkyl groups in alkylammonium-intercalated vermiculites. Besides, the MSDs of the alkyl groups in alkylammomonium-intercalated vermiculites with different carbon-chain lengths also varied from each other a little. This may be caused by the different densities of organic phases in the organoclays with different carbon-chain lengths.

The interlayer structures form a basis for investigating the sorption of small organic contaminants into organoclays, such as deducing the adsorption sites for organic pollutants. The low mobility of interlayer species indicates that the negatively charged surface of vermiculite can firmly fix groups with a positive charge. Based on this property, the inference can be made that vermiculite should be also able to fix other positively charged organics on its surface. These organics can be pollutants or the molecular groups used for the synthesis of advanced hybrid materials.

CONCLUSIONS

Molecular-dynamics simulations were performed to investigate the interlayer structures and dynamics of alkylammonium-intercalated vermiculites. The following conclusions were reached:

(1) The layering behavior of alkyl chains was established. The alkyl chains formed monolayers, bilayers, and pseudo-trimolecular layers as the carbon-chain length increased. The layering behaviors of alkyl chains were similar in alkylammonium-intercalated vermiculites and smectites, and they were controlled by both the amount of layer charge and the carbon-chain length.

(2) The ammonium groups had two locations: most ammonium groups were located above the six-member rings (~90%), and the rest were located above the substitution sites (~10%). In smectites, all ammonium groups were located above the six-member rings. This difference was caused by different layer-charge distributions in vermiculites and smectites.

https://doi.org/10.1346/CCMN.2017.064070 Published online by Cambridge University Press

(3) The ammonium groups had low mobility and the alkyl groups were slightly more mobile. This was similar to alkylammonium intercalated in smectites.

The results derived will be useful in further research into and in the applications of organo-vermiculites, *e.g.* in the synthesis of new hybrid materials and the removal of organic pollutants.

ACKNOWLEDGMENTS

The authors acknowledge the National Science Foundation of China (Nos. 41572027, 41425009, 41273074, and 41222015), the Special Program for Applied Research on Super Computation of the NSFC-Guangdong Joint Fund (the second phase) under Grant No. U1501501, the Fundamental Research Funds for the Central Universities (No. 020614380049), the Newton International Fellow Program, and the financial support from the State Key Laboratory for Mineral Deposits Research. They are grateful to the High Performance Computing Center (HPCC) of Nanjing University for doing the numerical calculations presented here, using its blade cluster system.

REFERENCES

Allen, M.P. and Tildesley, D.J. (1987) *Computer Simulation of Liquids*. Clarendon Press, Oxford, UK.

Al-Samhan, M., Samuel, J., Al-Attar, F., and Abraham, G. (2017) Comparative effects of MMT clay modified with two different cationic surfactants on the thermal and rheological properties of polypropylene nanocomposites. *International Journal of Polymer Science*, **2**, 1–8.

Bardziński, P.J. (2014) On the impact of intermolecular interactions between the quaternary ammonium ions on interlayer spacing of quat-intercalated montmorillonite: A molecular mechanics and *ab-initio* study. *Applied Clay Science*, **95**, 323–339.

Brigatti, M.F., Galán, E., and Theng, B. K.G. (2013) Structure and mineralogy of clay minerals. Pp. 21–81 in: *Handbook of Clay Science, 2nd Edition* (F. Bergaya and G. Lagaly, editors). Elsevier, Amsterdam.

Carrizosa, M.J., Rice, P.J., Koskinen, W.C., Carrizosa, I., and Hermosín, M.D. (2004) Sorption of isoxaflutole and DKN on organoclays. *Clays and Clay Minerals*, **52**, 341–349.

Chang, F.-R.C., Skipper, N.T., and Sposito, G. (1997) Monte Carlo and molecular dynamics simulations of interfacial structure in lithium-montmorillonite hydrates. *Langmuir*, **13**, 2074–2082.

Cygan, R.T. (2001) Molecular modeling in mineralogy and geochemistry. Pp. 1–35 in: *Molecular Modeling Theory: Applications in the Geosciences* (R.T. Cygan and J.D. Kubicki, editors). Reviews in Mineralogy and Geochemistry, **42**, Mineralogical Society of America. Washington, D.C.

Cygan, R.T., Liang, J.–J., and Kalinichev, A.G. (2004) Molecular models of hydroxide, oxyhydroxide, and clay phases and the development of a general force field. *Journal of Physical Chemistry B*, **108**, 1255–1266.

Dauber-Osguthorpe, P., Roberts, V.A., Osguthorpe, D.J., Wolff, J., Genest, M., and Hagler, A.T. (1988) Structure and energetics of ligand binding to proteins: *E. coli* dihydrofolate reductasetrimethoprim, a drug-receptor system. *Proteins: Structure, Function and Genetics*, **4**, 31–47.

Escamilla-Roa, E., Nieto, F., and Sainz-Díaz, C.I. (2016) Stability of hydronium cation in the structure of illite. *Clays and Clay Minerals*, **64**, 413–424.

Ferrage, E. (2016) Investigation of the interlayer organization of water and ions in smectite from the combined use of diffraction experiments and molecular simulations. A review of methodology, applications, and perspectives. *Clays and Clay Minerals*, **64**, 348–373.

Greenwell, H.C., Harvey, M.J., Boulet, P., Bowden, A.A., Coveney, P.V., and Whiting, A. (2005) Interlayer structure and bonding in nonswelling primary amine intercalated clays. *Macromolecules*, **38**, 6189–6200.

Gruner, J.W. (1934) The structures of vermiculites and their collapse by dehydration. *American Mineralogist*, **19**, 557–575.

Harvey, C.C. and Lagaly, G. (2013) Industrial applications. Pp. 451–490 in: *Handbook of Clay Science, 2nd Edition* (F. Bergaya and G. Lagaly, editors). Elsevier, Amsterdam.

He, H.P., Galy, J., and Gerard, J.F. (2005) Molecular simulation of the interlayer structure and the mobility of alkyl chains in HDTMA(+)/montmorillonite hybrids. *Journal of Physical Chemistry B*, **109**, 13301–13306.

Heinz, H., Koerner, H., Anderson, K.L., Vaia, R.A., and Farmer, B.L. (2005) Force field for mica-type silicates and dynamics of octadecylammonium chains grafted to montmorillonite. *Chemistry of Materials*, **17**, 5658–5669.

Janek, M. and Smrcok, L. (1999) Application of an internal standard technique by transmission X-ray diffraction to assess layer charge of a montmorillonite by using the alkylammonium method. *Clays and Clay Minerals*, **47**, 113–118.

Jankovič, Ľ., Kronek, J., Madejová, J., and Hronský, V. (2015) (9, 10-Dihydroxyoctadecyl)ammonium: A structurally unique class of clay intercalable surfactants. *European Journal of Inorganic Chemistry*, **17**, 2841–2850.

Kalinichev, A.G., Liu, X.D., and Cygan, R.T. (2016) Introduction to a special issue on molecular computer simulations of clays and clay-water interfaces: Recent progress, challenges, and opportunities. *Clays and Clay Minerals*, **64**, 335–336.

Lagaly, G. (1981) Characterization of clays by organic compounds. *Clay Minerals*, **16**, 1–21.

Lagaly, G. (1982) Layer charge heterogeneity in vermiculites. *Clays and Clay Minerals*, **30**, 215–222.

Lagaly, G., Ogawa, M., and Dekany, I. (2013) Clay mineral-organic interactions. Pp. 435–505 in: *Handbook of Clay Science, 2nd Edition* (F. Bergaya and G. Lagaly, editors). Elsevier, Amsterdam.

Laird, D.A., Scott, A.D., and Fenton, T.E. (1989) Evaluation of the alkylammonium method of determining layer charge. *Clays and Clay Minerals*, **37**, 41–46.

Lee, J.F., Mortland, M.M., Chiou, C.T., and Boyd, S.A. (1989) Shape-selective adsorption of aromatic molecules from water by tetramethylammonium-smectite. *Journal of the Chemical Society*, **85**, 2953–2962.

Li, Z.H., Jiang, W.T., and Hong, H.L. (2008) An FTIR investigation of hexadecyltrimethylammonium intercalation into rectorite. *Spectrochimica Acta Part A*, **71**, 1525–1534.

Liu, X.D., Lu, X.C., Wang, R.C., Zhou, H.Q., and Xu, S.J. (2007) Interlayer structure and dynamics of alkylammonium-intercalated smectites with and without water: A molecular dynamics study. *Clays and Clay Minerals*, **55**, 554–564.

Liu, X.D., Lu, X.C., Wang, R.C., Zhou, H.Q., and Xu, S.J. (2009) Molecular dynamics insight into the cointercalation of hexadecyltrimethyl-ammonium and acetate ions into smectites. *American Mineralogist*, **94**, 143–150.

Loewenstein, W. (1954) The distribution of aluminum in the tetrahedra of silicates and aluminates. *American Mineralogist*, **39**, 92–96.

Madejová, J., Sekeráková, Ľ., Bizovská, V., Slaný, M., and Jankovič, Ľ. (2016) Near-infrared spectroscopy as an effective tool for monitoring the conformation of alkylam-

https://doi.org/10.1346/CCMN.2017.064070 Published online by Cambridge University Press

monium surfactants in montmorillonite interlayers. *Vibrational Spectroscopy*, **84**, 44–52.

Mykola, S., Olga, N., and Dmitry, M. (2016) The influence of alkylammonium modified clays on the fungal resistance and biodeterioration of epoxy-clay nanocomposites. *International Biodeterioration & Biodegradation*, **110**, 136–140.

Nguemtchouin, M.G.M., Ngassoum, M.B., Kamga, R., Deabate, S., Lagerge, S., Gastaldi, E., Chalier, P., and Cretin, M. (2015) Characterization of inorganic and organic clay modified materials: An approach for adsorption of an insecticidal terpenic compound. *Applied Clay Science*, **104**, 110–118.

Osman, M.A., Seyfang, G., and Suter, U.W. (2000) Two-dimensional melting of alkane monolayers ionically bonded to mica. *Journal of Physical Chemistry B*, **104**, 4433–4439.

Osman, M.A., Ernst, M., Meier, B.H., and Suter, U.W. (2002) Structure and molecular dynamics of alkane monolayers self-assembled on mica platelets. *Journal of Physical Chemistry B*, **106**, 653–662.

Osman, M.A., Ploetze, M., and Skrabal, P. (2004) Structure and properties of alkylammonium monolayers self-assembled on montmorillonite platelets. *Journal of Physical Chemistry B*, **108**, 2580–2588.

Pazos, M.C., Cota, A., Osuna, F.J., Pavon, E., and Alba, M.D. (2015) Self-assembling of tetradecylammonium chain on swelling high charge micas (Na-Mica-3 and Na-Mica-2): Effect of alkylammonium concentration and mica layer charge. *Langmuir*, **31**, 4394–4401.

Perry, T.D., Cygan, R.T., and Mitchell, R. (2006) Molecular models of alginic acid: Interactions with calcium ions and calcite surfaces. *Geochimica et Cosmochimica Acta*, **70**, 3508–3532.

Sarkar, M., Dana, K., and Ghatak, S. (2011) Evolution of molecular structure and conformation of n-alkylammonium intercalated iron rich bentonites. *Journal of Molecular Structure*, **1005**, 161–166.

Scholtzová, E., Madejová, J., Jankovič, L., and Tunega, D. (2016) Structural and spectroscopic characterization of montmorillonite intercalated with n-butylammonium cations (*N*=1-4)-modeling and experimental study. *Clays and Clay Minerals*, **64**, 401–412.

Smith, W. and Forester, T.R. (1996) DL_POLY_2.0: A general-purpose parallel molecular dynamics simulation package. *Journal of Molecular Graphics*, **14**, 136–141.

Szczerba, M., Kuligiewicz, A., Derkowski, A., Gionis, V., Chryssikos, G.D., and Kalinichev, A.G. (2016) Structure and dynamics of water-smectite interfaces: Hydrogen bonding and the origin of the sharp O-Dw/O-Hw infrared band from molecular simulations. *Clays and Clay Minerals*, **64**, 452–471.

Tambach, T.J., Boek, E.S., and Smit, B. (2006) Molecular order and disorder of surfactants in clay nanocomposites. *Physical Chemistry Chemical Physics*, **8**, 2700–2702.

Vaia, R.A., Teukolsky, R.K., and Giannelis, E.P. (1994) Interlayer structure and molecular environment of alkylammonium layered silicates. *Chemistry of Materials*, **6**, 1017–1022.

Wang, L.Q., Liu J., Exarhos, G.J., Flanigan, K.Y., and Bordia, R. (2000) Conformation heterogeneity and mobility of surfactant molecules in intercalated clay minerals studied by solid-state NMR. *Journal of Physical Chemistry B*, **104**, 2810–2816.

Weiss, A. (1963) Organic derivatives of mica-type layer silicates. *Angewandte Chemie International Edition*, **2**, 134–144.

Wen, X.Y., He, H.P., Zhu, J.X., Jun, Y., Ye, C.H., and Deng, F. (2006) Arrangement, conformation, and mobility of surfactant molecules intercalated in montmorillonite prepared at different pillaring reagent concentrations as studied by solid-state NMR spectroscopy. *Journal of Colloid and Interface Science*, **299**, 754–760.

Zeng, Q.H., Yu, A.B., Lu, G.Q., and Standish, R.K. (2003) Molecular dynamics simulation of organic-inorganic nanocomposites: the layering behavior and interlayer structure of organoclays. *Chemistry of Materials*, **15**, 4732–4738.

Zeng, Q.H., Yu, A.B., Lu, G.Q., and Standish, R.K. (2004) Molecular dynamics simulation of the structural and dynamic properties of organoclay. *Journal of Physical Chemistry B*, **108**, 10025–10033.

Zhao, Q. and Burns, S.E. (2012) Molecular dynamics simulation of secondary sorption behavior of montmorillonite modified by single chain quaternary ammonium cations. *Environmental Science & Technology*, **46**, 3999–4007.

Zhu, J.X., He, H.P., Zhu, L.Z., Wen, X.Y., and Deng, F. (2005) Characterization of organic phases in the interlayer of montmorillonite using FTIR and C-13 NMR. *Journal of Colloid and Interface Science*, **286**, 239–244.

(*Received 25 July 2017; revised 06 October 17 2017; Ms. 1191; AE: Chun-Hui Zhou*)

https://doi.org/10.1346/CCMN.2017.064070 Published online by Cambridge University Press